J Nanostruct 13(3): 718-728, Summer 2023

RESEARCH PAPER

# Electropolymerization of DPC and DPC-Metal Oxides Nanocomposites on Low Carbon Steel and Evaluating their Corrosion Protection Performance

*Zainab Hussain* *, *Khulood A.Saleh*

[1] *Department of Chemistry, College of Science, University of Baghdad, Baghdad, Iraq*

ARTICLE INFO

*Article History:*
*Received 07 March 2023*
*Accepted 23 May 2023*
*Published 01 July 2023*

*Keywords:*
*Corrosion*
*Low Carbon Steel*
*Electrochemical polymerization*
*Nanocomposite*
*Tafel*

ABSTRACT

This study is concerned with the synthesis and characterization of new Conductive polymer films (3830 µs/cm) poly 6-((1,5-dimethyl-3-oxo-2-phenyl-2,3-dihydro-1*H*-pyrazol-4-yl)carbamoyl) cyclohex-3-ene-1-carboxylic acid (PDPC) on the surface of low carbon steel electrode (L.C.S), which were synthesized starting from 6-((1,5-dimethyl-3-oxo-2-phenyl-2,3-dihydro-1*H*-pyrazol-4-yl)carbamoyl) cyclohex-3-ene-1-carboxylic acid (DPC) as a monomer by electropolymerization method. Also, the ability of this polymeric coating to protect the surface from corrosion was tested in a saline solution 3.5% NaCl at various temperatures ranging from (298 to 328)K using a potentiostat that measures the corrosion rate by plotting Tafel lines. The new polymer-nanocomposites were also synthesized by adding nanometal-oxides: Zirconium dioxide ($ZrO_2$) or Magnesium oxide (MgO) to the monomer solution to improve the anticorrosion properties of the prepared polymeric films. The functional groups, phase composition, and morphology of the prepared coatings were investigated using a Fourier Transform Infrared (FTIR) analysis, X-ray diffraction (XRD), and Atomic Force Microscopy (AFM). The examination of kinetic and thermodynamic activation parameters ($E_a$, A, $\Delta H^*$, and $\Delta S^*$) showing data results that the activation energies of L.C.S corrosion increased after coating due to the increasing energy barrier for the corrosion process and the best protection efficiency was 90.4 % at 298 K in case of using PDPC-$ZrO_2$ nanocomposite as a coating.

**How to cite this article**
*Hussain Z, Saleh K A. Electropolymerization of DPC and DPC-Metal Oxides Nanocomposites on Low Carbon Steel and Evaluating their Corrosion Protection Performance. J Nanostruct, 2023; 13(3):718-728. DOI: 10.22052/JNS.2023.03.013*

## INTRODUCTION

Researchers have increasingly concentrated on studying corrosion behavior and its mechanism in metal materials to support the development of preventative measures and technologies against it. It is a crucial process affecting economics and safety, particularly for metals and alloys [1-2]. Low carbon steel is an alloy of iron and carbon, the latter containing up to about 0.25 - 0.3 carbon by weight of its composition. Generally, it is neither brittle nor ductile, and its microstructure consisted mainly of ferrite and perlite. Due to its ease of manufacture, good availability, and relatively low price, this type of steel is the base material to be used in various applications - in automobile body panels, bolts, fixtures, seamless tubes, and steel plates [3]. Corrosion of low carbon steel and the formation of corrosion products like iron oxides is one of the factors that obstruct the wide range of usage [4]. For this reason, the study of the formation of polymeric films on oxidizable metals by electropolymerization in aqueous media has been widely studied in recent years, with attention mainly to electron-conducting polymers obtained

* *Corresponding Author Email: zainab_alaa@ymail.com*

by electrooxidation of aniline, pyrrole, pyridine, thiophene, and other monomers that have capable of acquiring positive or a negative charge through oxidation or reduction [5-6]. The properties of these polymeric coatings depend largely on the electropolymerization conditions: solvent, electrolyte, pH, monomer concentration, metallic substrate nature, electrochemical treatment, etc. [6].

The electrochemical polymerization techniques are divided into three types: potentiostatic ( using a constant voltage), galvanostatic ( using a constant current) and cyclic voltammetry (by using cyclic uniform change of the potential). Three metallic electrodes are used: the working electrode (the metal or alloy to be protected from corrosion), the reference electrode (often a calomel electrode), and the auxiliary electrode (platinum electrode).

The medium of the reaction can have just as much of an impact as the monomer. Most organic solvents, including alcohols, glycols, DMF, nitrobenzene, acetone, acetonitrile, and dichloromethane are suitable for the procedure. Using water as a solvent has clear practical benefits. In addition to being inexpensive, it is also non-toxic and avoids fire risk. However, in some cases, adding additional methanol (or stronger alcohols) may be required to produce sufficient solubility of the monomers [7]. Furthermore, nanoparticle Polymer composites are the best alternative to traditional polymer fillers due to their nano-size and dispersion of fillers, which enhance their properties and make them unique and distinctive for use in various applications like the inhibition of metal corrosion [8].

Therefore, this study attempted to synthesize a conductive polymer film (PDPC) to protect L.C.S from corrosion in a saline solution (3.5% NaCl) at a temperature ranging between (298-328)K using an electropolymerization process, and the impact of adding nanometal oxides ($ZrO_2$ and MgO) for the polymeric coating to increase the corrosion protection efficiency.

## MATERIALS AND METHODS

*Metal Sample Preparation*

The L.C.S plate used in this work, with an area of 2×2 $cm^2$ and a thickness of 15 mm, was cut into discs 25 mm in diameter. These plates were polished with silicon carbide metallic paper of different grades, such as 180, 220, 400, 1200, 2000, and 2500 mesh grit, washed with tap water and distilled water, degreased with acetone, and then cleaned with absolute ethanol before being dried with a heat gun and kept in a desiccator [9–10].

*Electropolymerization Technique*

To electropolymerize of the monomer 6-((1,5-dimethyl-3-oxo-2-phenyl-2,3-dihydro-1*H*-pyrazol-4-yl)carbamoyl)cyclohex-3-ene-1-carboxylic acid (DPC), two electrodes were used: an L.C.S. disc served as the working electrode. In contrast, a stainless steel plate served as the counter electrode using a *DC-power supply*. The coating solution for electropolymerization consisted of 0.1g (0.003 M) of DPC monomer in 100 ml of distillate water with three drops of $H_2SO_4$. An estimated voltage of (1.5 V) was applied at room temperature for (45 min), then the coated

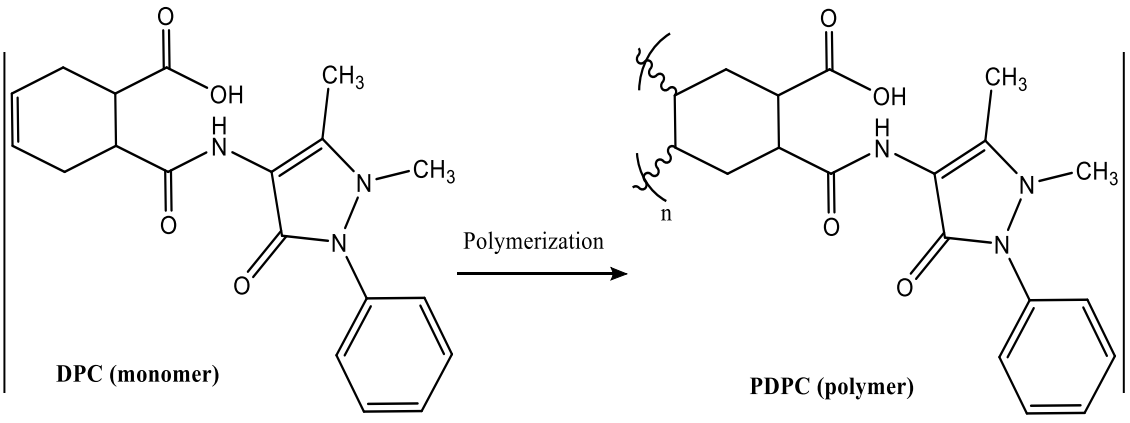


Fig. 1. Synthesis of PDPC polymer.

electrode was dried by a heat gun. Furthermore, to improve the effectiveness of the polymer films in protecting L.C.S against corrosion, 40 and 50 ppm of the nanometal oxides $ZrO_2$ or MgO were added, respectively. Fig. 1 illustrates DPC's electropolymerization.

*Study of Corrosion*

The corrosion protection properties of the coating were investigated using the Tafel polarization technique. For corrosion measurements, LCS was used as a working electrode, platinum was used as an auxiliary electrode, and saturated calomel as a reference electrode. In a saline solution (3.5% NaCl) at a temperature ranging from (298 to 328) K, cathodic and anodic polarization of L.C.S were carried out under potentiostatic conditions[12].

## RESULTS AND DISCUSSIONS

*Suggested Mechanism of Polymerization of DPC on L.C.S Electrode*

The cationic polymerization method, which occurs in the following phases as detailed below

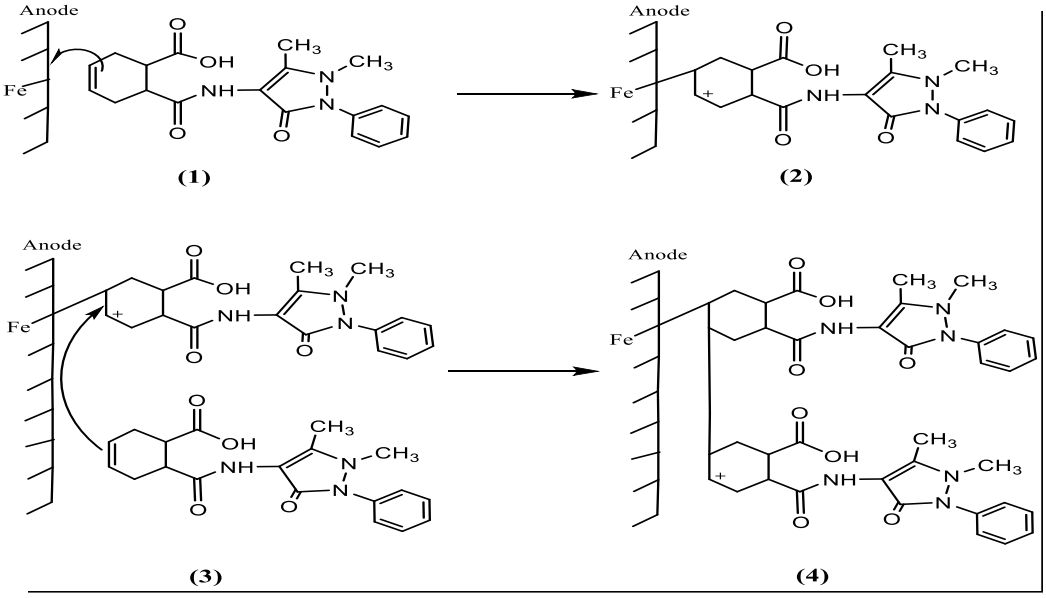


Fig. 2. Suggested Mechanism of Polymerization of DPC on L.C.S electrode.

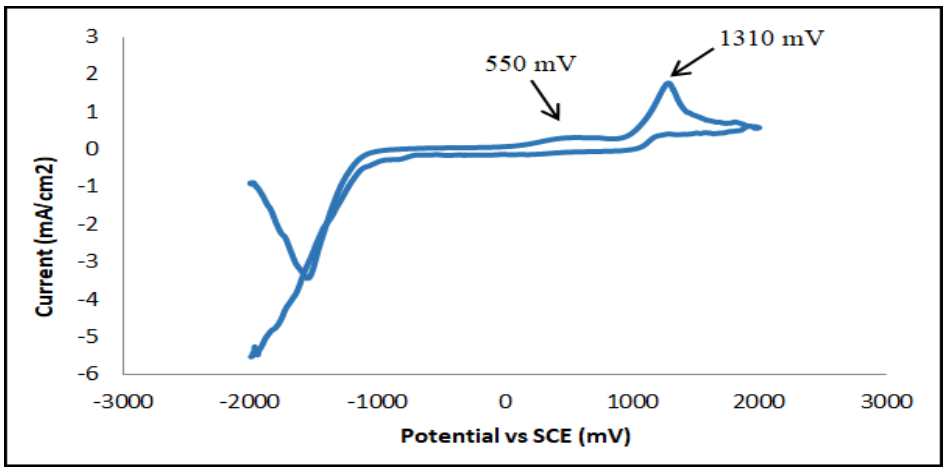


Fig. 3. Cyclic voltammogram of the electropolymerization of DPC monomer on the L.C.S

[13], was used to electropolymerize a DPC monomer on the L.C.S electrode surface.

1. When an anodic potential is supplied to a monomer solution, an electron will go from the monomer to the electrode, forming a cationic radical adsorbed on the electrode's surface, as shown in steps 1 to 2 of Fig. 2.

2. In order to increase the molecular weight of the species, the generated cationic radicals were desorbed and reacted in the solution. Next, the monomer molecules are added using a cationic addition mechanism at the charged end of the oxidized monomer, as indicated in steps 3 to 4 of Fig. 2.

*Electropolymerization of DPC with cyclic voltammetry*

A cyclic voltammogram of the PDPC film deposited on L.C.S electrode in saline solution (3.5% NaCl) in the potential range between -2000 to +2000 mV vs. SCE is shown in Fig. 3. The voltammogram shows a distinctive anodic peak in the anodic excursion, around 1310 mV, and another very small one, around 550 mv. It can be seen from this scan that the oxidation wave starts at about 1310 mV. This indicates that an irreversible oxidation reaction of the monomer occurred on the surface of the electrode, in which cationic radicals were activated, leading to the

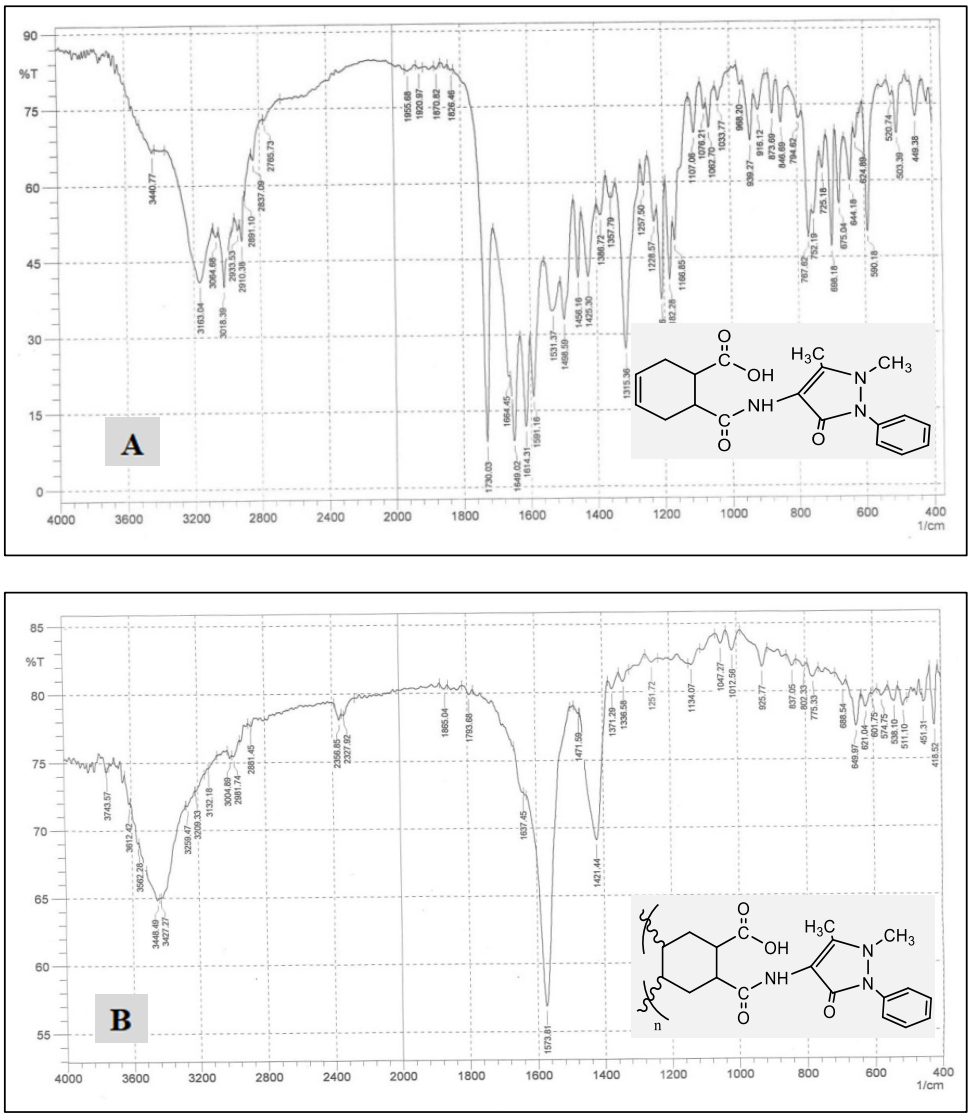


Fig. 4. FTIR spectra of (A) DPC and (B) PDPC.

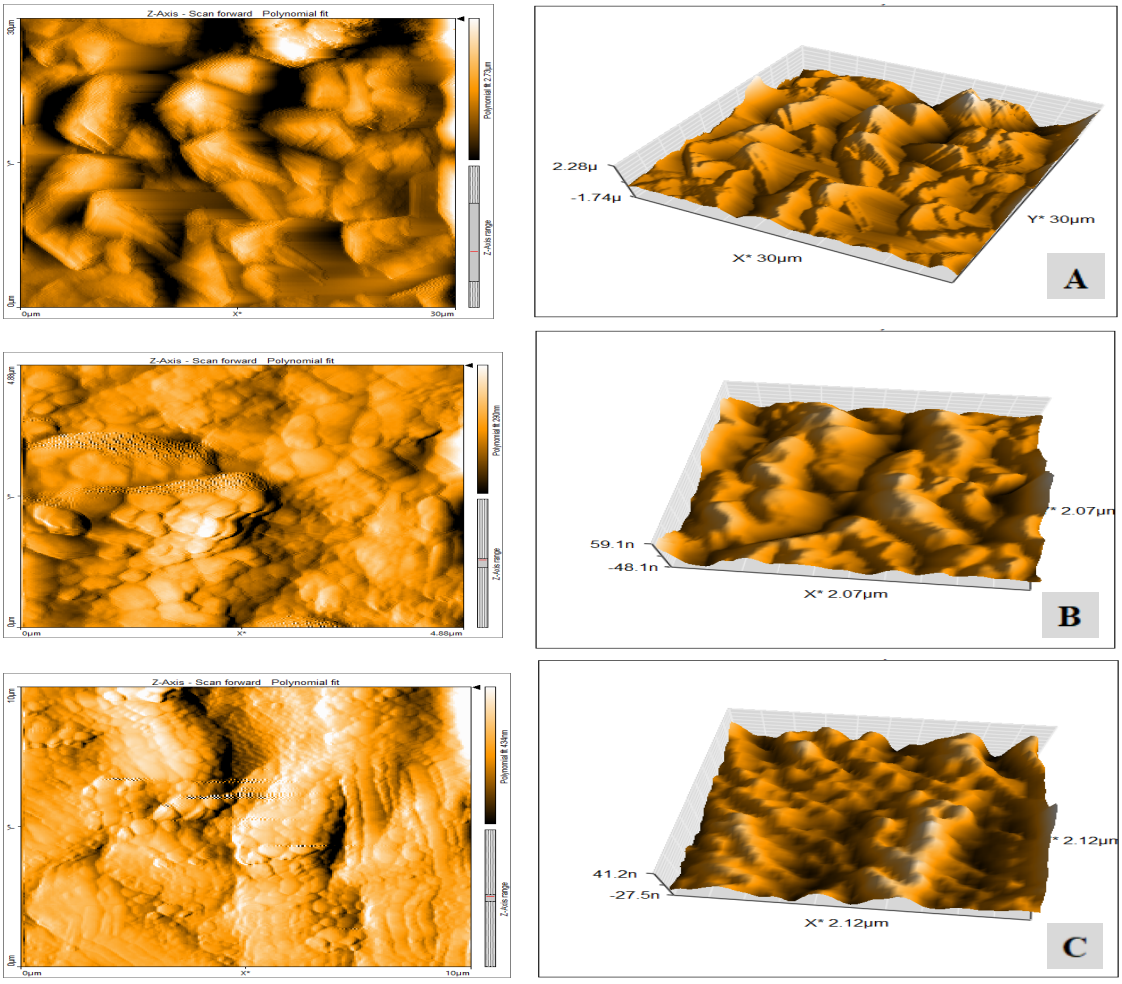


Fig. 5. AFM images of (A) L.C.S coated with PDPC, (B) L.C.S coated with PDPC-$ZrO_2$ nanocomposite, (C) L.C.S coated with PDPC-MgO nanocomposite.

Table 1. The mean grain size, average roughness, and root mean square roughness for L.C.S coated with PDPC films in the absence and presence of nanometal oxides.

| System | Ra (nm) | RMS (nm) | Main grain size (nm) |
|---|---|---|---|
| PDPC | 712.4 | 839.3 | 306.3 |
| PDPC-$ZrO_2$ nanocomposite | 33.44 | 45.09 | 112.8 |
| PDPC-MgO nanocomposite | 60.37 | 77.48 | 93.12 |

electropolymerization reaction. After repetitive cycles, a light brownish polymer coating is revealed. Increases in anodic current were attributed to the polymer's electropolymerization [15].

*Characterization of the electropolymerization of DPC by FTIR spectroscopy*

The (FTIR) spectrum of the synthesized polymer (PDPC) and its monomer (DPC) was recorded to predict the structure and functional groups present in the polymer formed on the L.C.S electrode surface, as evident in Fig. 4.

The spectrum of FTIR in Fig. 2-A for the monomer shows stretching bands at 3440.7 $cm^{-1}$ for carboxylic OH, 3163 $cm^{-1}$ for NH, and 3018 $cm^{-1}$ for aromatic C-H. The C=O carboxylic acid and C=O amide groups appeared at 1730 and 1664.45 $cm^{-1}$, respectively; also, a band at 1614.3 $cm^{-1}$ may be attributed to C=C aromatic ring. The disappearance of the double bond (C=C) olefinic groups in Fig.

2-B indicates that the polymer PDPC has formed. The transmission peak is comparatively broad due to the polymer PDPC having abroad chain distribution [16].

*Atomic Force Microscopy Analysis*

Atomic Force Microscopy (AFM) has been used to give a topographical image of the surface of L.C.S coated with PDPC films in both the presence and absence of nanometal oxides.

The prepared polymer's two and three dimensions are depicted in Fig. 5(A, B, and C) in both the absence and presence of the nanometal oxides. These images demonstrate the degree of nanomaterial aggregation brought about by $ZrO_2$ and MgO adhering to the polymer and forming the smooth layers. Average roughness (Ra) and root mean square roughness (RMS) are two of the measures that are most frequently used in AFM analysis to define the surface roughness of the produced polymer films. The obtained RMS and Ra values are listed in Table (1). The results show a reduction in surface roughness (increase in smoothness) following the polymer's treatment with nanometal oxides due to the decrease in grain size [17].

*Scanning Electrons Microscopes (SEM) Analysis*

SEM images represent the morphology of a sample and can also reconstruct quasi-three dimensional views of the sample surface. Therefore, the technique was used to study the surface morphology of the L.C.S coated with PDPC films in both the presence and absence of nanometal oxides [18]. Fig. 6(A, B, and C) compares the SEM images of pure PDPC (Fig. 6A) and PDPC with nanometal oxides (Fig. 6 (B and C)). As can be seen, the pure PDPC coating has a completely different morphology compared with PDPC-$ZrO_2$ and MgO nanocomposites coatings. Fig. 6A shows that the PDPC film has a bulky and porous appearance, which paves more pathways

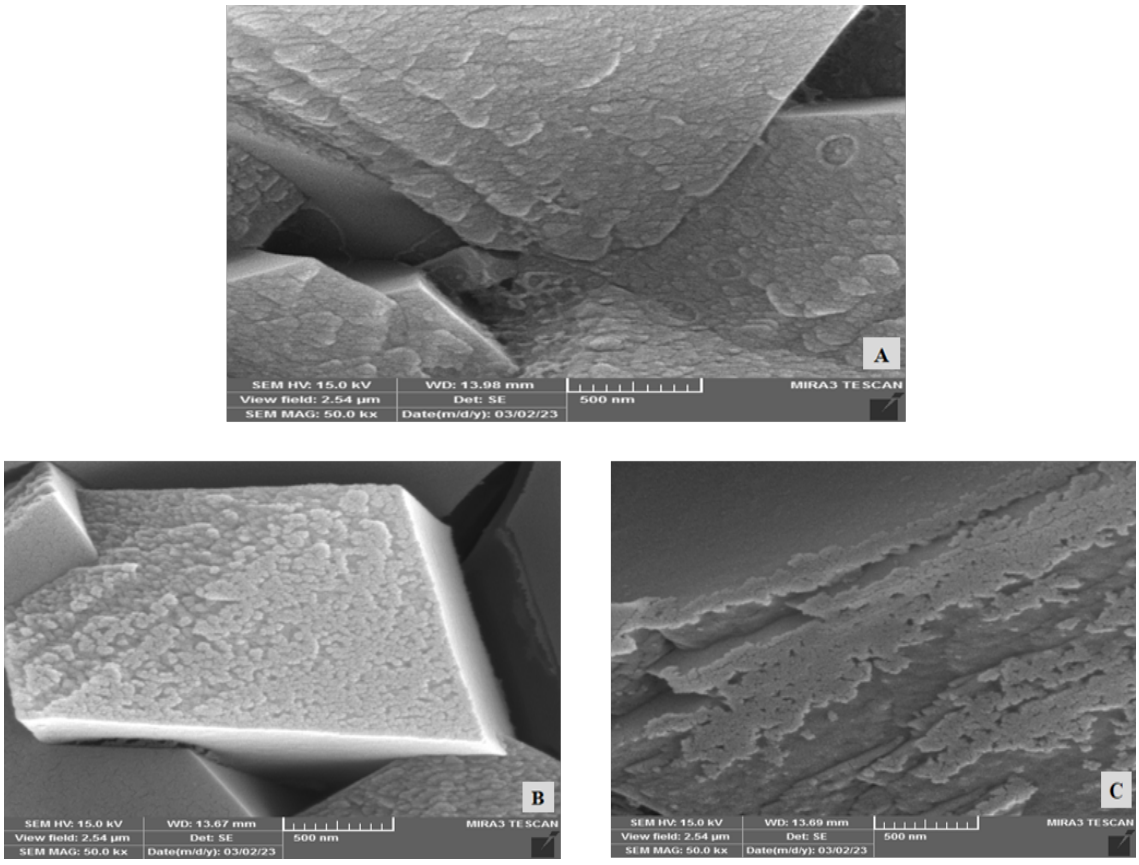


Fig. 6. SEM images of (A) L.C.S coated with PDPC, (B) L.C.S coated with PDPC-$ZrO_2$ nanocomposite, (C) L.C.S coated with PDPC-MgO nanocomposite.

for the electrolyte to reach the metal surface under the coating with an irregular distribution on the L.C.S. surface. Fig. 6B depicts the surface of L.C.S coated with PDPC-$ZrO_2$ nanocomposite; it is illustrated from this Fig. that the surface became smoother and more covered due to the high specific surface area, and the distribution of the coating has become more uniform compared with the pure polymer. 6C depicts the surface of L.C.S covered with PDPC-MgO nanocomposite, in this Figure, we can see the uniform distribution and strong interaction between the surface of L.C.S and the modified polymer matrix [19].

*Corrosion tests*

Tafel curves were used to find out the effect of the polymeric coating layers formed on the L.C.S alloy in protecting the alloy from corrosion by knowing the changes that occur in the corrosion current of the alloy immersed in a saline solution (3.5% NaCl) at a range of temperatures between (298 and 328) K. The Tafel curves ( 7) were plotted using a potentiostat, and from these curves, we can obtain the corrosion potential ($E_{corr}$), cathodic Tafel slope ($B_c$), anodic Tafel slope ($B_a$), corrosion current density ($i_{corr}$), weight loss (W.L), and penetration loss (P.L) listed in Table (2). From this

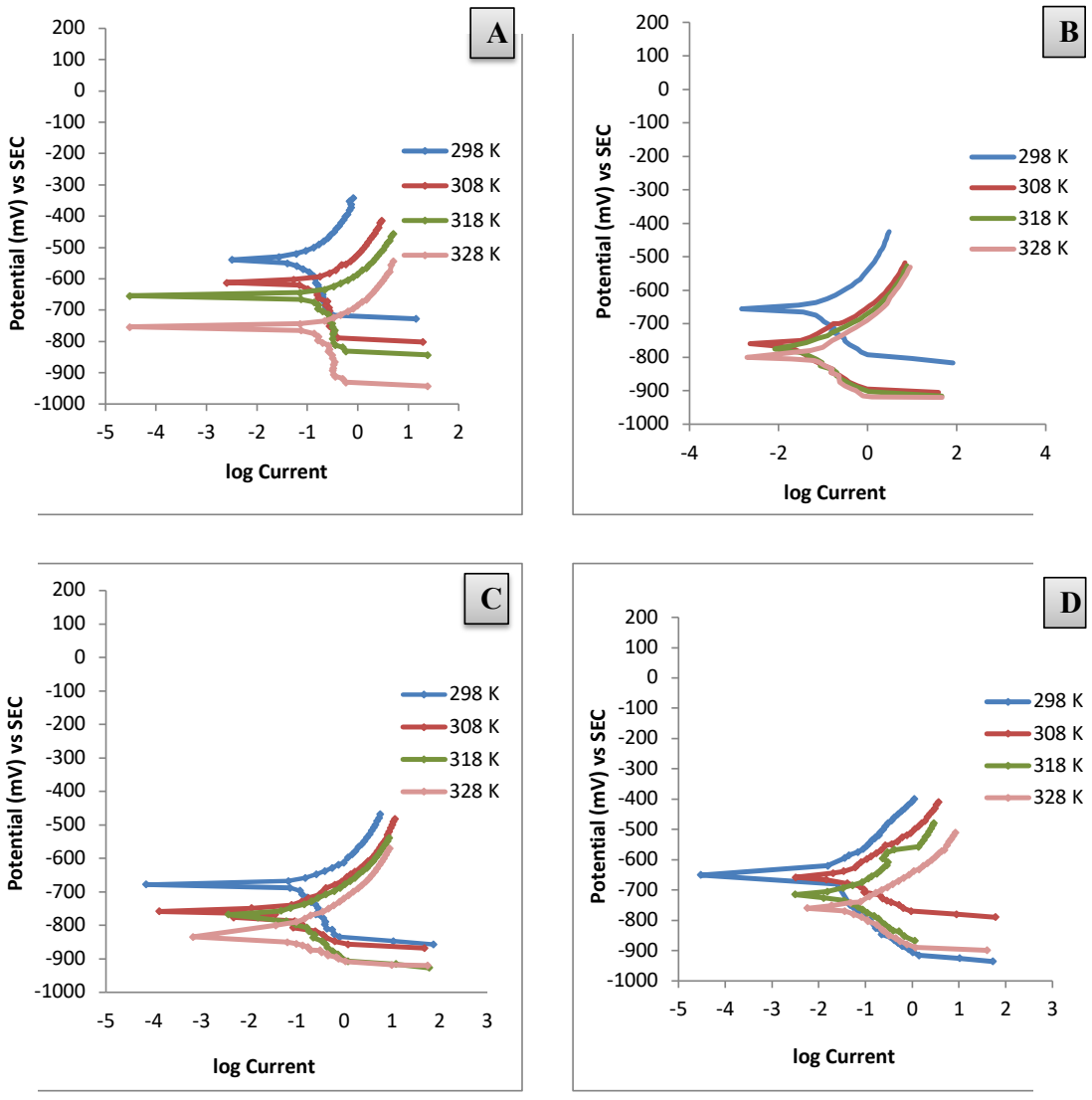


Fig. 7. Polarization diagrams for (A) uncoated L.C.S, (B) L.C.S coated with PDPC, (C) L.C.S coated with PDPC-$ZrO_2$ nanocomposite and (D) L.C.S coated with PDPC–MgO nanocomposite.

Table 2. Corrosion parameters for L.C.S coated and uncoated with PDPC in the presence and absence of nanometal oxides in a saline solution (3.5% NaCl) at different temperatures.

| System | T (K) | $E_{corr}$ (mV) | $i_{corr}$ (μA/cm²) | $\beta c$ (mV/Dec) | $\beta a$ (mV/Dec) | WL (mm/y) | PL (g/m².d) | PE% | $R_p$ (Ω/cm²) |
|---|---|---|---|---|---|---|---|---|---|
| Uncoated L.C.S | 298 | -530.0 | 63.51 | -142.1 | 104.8 | 1.590 | 0.737 | - | 412.38 |
| | 308 | -610.0 | 76.20 | -145.1 | 120.0 | 1.900 | 0.885 | - | 374.27 |
| | 318 | -650.0 | 117.69 | -239.4 | 80.1 | 2.940 | 1.370 | - | 221.43 |
| | 328 | -691.1 | 141.82 | -449.6 | 70.9 | 3.550 | 1.650 | - | 187.50 |
| L.C.S coated with PDPC | 298 | -655.4 | 18.70 | -90.1 | 78.9 | 0.468 | 0.217 | 70.5 | 976.74 |
| | 308 | -760.0 | 22.94 | -161.3 | 74.5 | 0.573 | 0.266 | 69.8 | 964.60 |
| | 318 | -775.3 | 38.08 | -110.0 | 76.3 | 0.952 | 0.442 | 67.6 | 513.70 |
| | 328 | -855.1 | 49.53 | -118.3 | 77.4 | 0.985 | 0.575 | 65.0 | 410.17 |
| L.C.S coated with PDPC +$ZrO_2$ Nanocomposite | 298 | -677.4 | 8.88 | -92.0 | 55.0 | 0.222 | 0.103 | 85.0 | 1683.16 |
| | 308 | -758.8 | 12.60 | -65.5 | 55.2 | 0.315 | 0.146 | 83.0 | 1032.30 |
| | 318 | -768.0 | 25.69 | -67.0 | 151.2 | 0.642 | 0.298 | 78.0 | 784.71 |
| | 328 | -770.0 | 35.35 | -82.1 | 56.2 | 0.884 | 0.410 | 75.0 | 408.93 |
| L.C.S coated with PDPC +MgO Nanocomposite | 298 | -650.0 | 6.08 | -43.8 | 71.3 | 0.152 | 0.070 | 90.4 | 1937.71 |
| | 308 | -658.8 | 12.37 | -85.8 | 70.1 | 0.309 | 0.144 | 83.8 | 1354.23 |
| | 318 | -715.0 | 21.37 | -82.4 | 73.8 | 0.534 | 0.248 | 81.8 | 791.05 |
| | 328 | -760.0 | 27.94 | -74.1 | 81.5 | 0.698 | 0.324 | 80.2 | 603.17 |

information obtained from the Tafel curves, the protection efficiency (PE%) can be calculated using the following equation (1):

$$PE\% = \frac{i_{corr,uncoated} - i_{corr,coated}}{i_{corr,uncoated}} \times 100\% \quad (1)$$

Where: $i_{corr,\ coated}$, $i_{corr,\ uncoated}$ are the corrosion current densities for coated and uncoated L.C.S, respectively. The Stern-Gery equation (equation 2) was used to compute the polarization resistance (Rp) as well [20]:

$$R_p = \frac{B_a|B_c|}{2.303(B_a + |B_c|)i_{corr}} \quad (2)$$

Similar to full polarization curve measurements, polarization resistance ($R_p$) tests are useful for locating corrosion problems and launching corrective action [21]. The values are shown in Table 2.

*Kinetic and Thermodynamic Activation Parameters of Corrosion*

Corrosion of L.C.S. in a saline solution (3.5% NaCl) can be affected by temperature. Potentiostatic measurements were performed at various temperatures (298 to 328) K both in the absence and presence of PDPC and PDPC-metal oxides nanocomposite to estimate the activation energy of the corrosion process. The Arrhenius equations (3, 4) were applied to the activated complex generated in the transition state to calculate the corrosion process's activation parameters [22]. Table 3 and Figs. 8 and 9 show the results.

$$\log C.R = \log A - \frac{E_a}{2.303\ RT} \quad (3)$$

$$\log \frac{C.R}{T} = \log\left(\frac{R}{Nh}\right) + \frac{\Delta S^*}{2.303\ R} - \frac{\Delta H^*}{2.303RT} \quad (4)$$

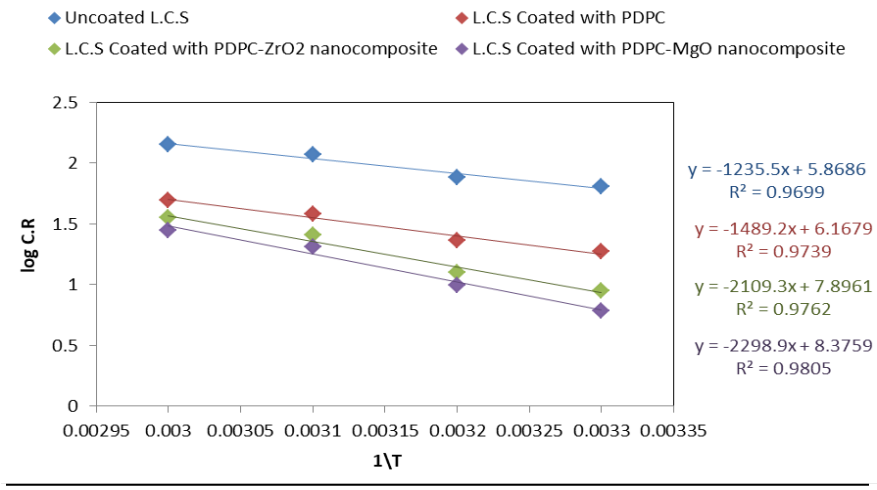


Fig. 8. The relationship between log C.R & (1\T) of L.C.S coated and uncoated with PDPC with and without nanometal oxides in a saline solution (3.5% NaCl).

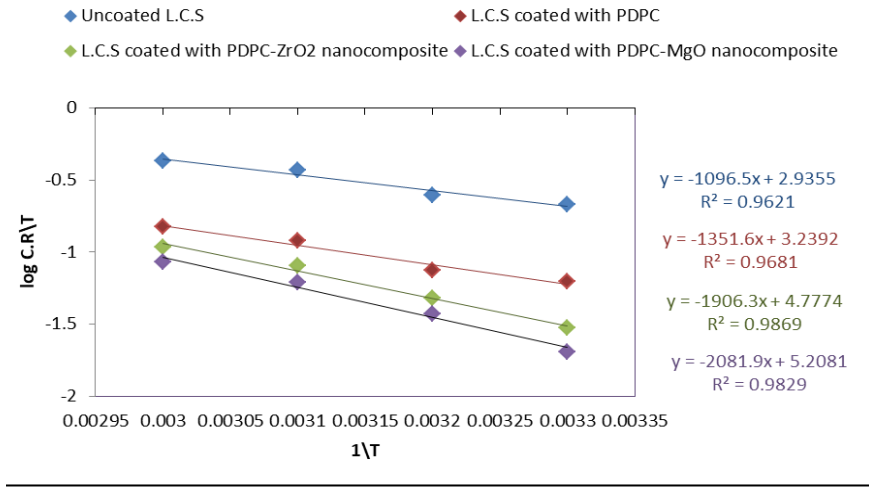


Fig. 9. The relationship between log (C.R\T) & (1\T) of L.C.S coated and uncoated with PDPC with and without nanometal oxides in a saline solution (3.5% NaCl)

Where: A is the Arrhenius preexponential factor, T is the absolute temperature (K), R is the molar gas constant ($JK^{-1}mol^{-1}$), $E_a$ is the apparent effective activation energy, C.R is the corrosion rate, which is equal to the corrosion current density, N is Avogadro's number, and h is the Planck constant.

The activation energy (Ea) and the Arrhenius preexponential factor (A) were calculated using a linear regression between log C.R and 1/T, as shown in 8. The current study shows that the value of A in the presence of PDPC and PDPC-metal oxide nanocomposite is larger than that in their absence; hence, the apparent activation energy determines the decline in L.C.S corrosion rate. This rise in the values of Ea in the presence of PDPC and PDPC-metal oxide nanocomposite can be related to an increase in the double-layer thickness, which raises the corrosion process's Ea [23]. It also indicates a strong protective action

Table 3. Kinetic and thermodynamic activation parameters for L.C.S coated and uncoated with PDPC at various temperatures, with and without nanometal oxides.

| System | $E_a^*$ (kJ\mol) | A (Molecule .cm$^{-2}$. S$^{-1}$) | $\Delta H^*$ (kJ\mol) | $\Delta S^*$ (J/mol. K) |
|---|---|---|---|---|
| Uncoated L.C.S | 23.656 | $4.448\times10^{29}$ | 20.994 | -141.373 |
| L.C.S coated with PDPC | 28.513 | $8.861\times10^{29}$ | 25.879 | -135.558 |
| L.C.S coated with PDPC-$ZrO_2$ nanocomposite | 40.387 | $4.739\times10^{31}$ | 36.500 | -106.106 |
| L.C.S coated with PDPC-MgO nanocomposite | 44.017 | $1.430\times10^{32}$ | 39.862 | -97.859 |

of PDPC and PDPC-metal oxides nanocomposite by increasing the energy barrier for the corrosion process with highlighting the electrostatic nature of the polymer adsorption (physisorption) on the L.C.S surface [24].

Straight lines with a slope of (ΔH*/2.303R) and an intercept of [log (R/Nh)+(ΔS*/2.303R)] were derived using plots that show the correlation between the reciprocal of absolute temperature (1/T) and log (C.R/T) ( 9) from which the values of ΔH* and ΔS*respectively were computed and also listed in Table 3. The positive values of ΔH* in the absence and presence of the coating layer reflect the endothermic nature of the L.C.S dissolution process. It can also be seen from Table 3 that the values of activation energy and activation enthalpy diversified in the same manner. This result verified the known thermodynamic relation between $E_a$ and ΔH* [25]. The negative values of the entropy of activation in the absence and presence of the coating layer imply that the activated complex in the rate-determining step represents an association rather than a dissociation step, meaning that a decrease in disordering takes place in going from reactants to the activated complex [26].

## CONCLUSION

Electropolymerization of DPC monomer was carried out to produce PDPC polymeric films on the surface of L.C.S alloy, which is used as coatings to protect it from corrosion. The results showed that these prepared polymeric films provide good protection for L.C.S against corrosion in saline medium (3.5%NaCl), and the efficiency of this protection decreases with increasing temperature. The efficiency of the prepared polymeric films in protecting the L.C.S from corrosion increases by adding oxides of nanomaterial such as ($ZrO_2$ and MgO). The best protection efficiency was 90.4% at 298 K when using PDPC-$ZrO_2$ nanocomposite as a coating. Finally, The kinetic and thermodynamic study showed that the activation energies of L.C.S corrosion increased after coating due to the increasing energy barrier for the corrosion process.

## CONFLICT OF INTEREST

The authors declare that there is no conflict of interests regarding the publication of this manuscript.

## REFERENCES

1. Afia L, Hamed O, Larouj M, Lgaz H, Jodeh S, Salghi R. Novel Natural Based Diazepines as Effective Corrosion Inhibitors for Carbon Steel in HCl Solution: Experimental, Theoretical and Monte Carlo Simulations. Transactions of the Indian Institute of Metals. 2017;70(9):2319-2333.
2. Keywords. Corros Sci. 2002;44(12):XXIX-XXX.
3. Stambolova I, Boshkov NS, Boshkova N, Stoyanova D, Shipochka M, Simeonova S, et al. Environmentally-Friendly Anticorrosive Layered Zirconia/Titania/Low-Carbon Steel Structures. The 2nd International Online-Conference on Nanomaterials; 2020/11/15: MDPI; 2020.
4. International Journal of Innovative Research in Advanced Engineering.
5. Sitorus B, Malino MB. Electrical Conductivity of Conducting Polymer Composites based on Conducting Polymer/Natural Cellulose. ELKHA. 2021;13(1):84.
6. Garcés P, Lapuente R, Andión LG, Cases F, Morallón E, Vázquez JL. Electropolymerization of Phenol on Carbon Steel and Stainless Steel Electrodes in Carbonate Aqueous Medium. Polym J. 2000;32(8):623-628.
7. Samet Y, Kraiem D, Abdelhédi R. Electropolymerization of phenol, o-nitrophenol and o-methoxyphenol on gold and carbon steel materials and their

corrosion protection effects. Prog Org Coat. 2010;69(4):335-343.
8. Sharma K, Goyat MS, Vishwakarma P. Synthesis of Polymer Nano-composite coatings as corrosion inhibitors: A quick review. IOP Conference Series: Materials Science and Engineering. 2020;983(1):012016.
9. Al-Rudaini KAK, Al-Saadie KAS. Milk Thistle Leaves Aqueous Extract as a New Corrosion Inhibitor for Aluminum Alloys in Alkaline Medium. Iraqi Journal of Science. 2021:363-372.
10. Fomo G, Waryo T, Feleni U, Baker P, Iwuoha E. Electrochemical Polymerization. Polymers and Polymeric Composites: A Reference Series: Springer International Publishing; 2019. p. 105-131.
11. Khalaf MI, Saleh KA, Khalil KS. Novel Electro Polymerization Method to Synthesized Anti-corrosion Coated Layer on Stainless Steel Surface from (N-Benzothiazolyl Maleamic Acid) and Study its Biological Activity. International Journal of Pharmaceutical Quality Assurance. 2018;9(3).
12. Saleh KA, Ali MI. Electro polymerization for (N-Terminal tetrahydrophthalamic acid) for Anti-corrosion and Biological Activity Applications. Iraqi Journal of Science. 2020:1-12.
13. Zare EN, Lakouraj MM, Moosavi E. Poly (3-aminobenzoic acid) @ MWCNTs hybrid conducting nanocomposite: preparation, characterization, and application as a coating for copper corrosion protection. Compos Interfaces. 2016;23(7):571-583.
14. Sayyah SM, Abd El-Rehim SS, El-Deeb MM. Electropolymerization of pyrrole and characterization of the obtained polymer films. J Appl Polym Sci. 2003;90(7):1783-1792.
15. Abbas Mohammed R, Saleh KA. Advanced anticorrosive coating prepared from poly [N-(Pyridine-2-yl) maleamic acid]/graphene derivatives nanocomposites. Materials Today: Proceedings. 2022;61:805-812.
16. Alqudsi AM, Saleh KA. Conducting Polyanethole / Metals Oxides Nanocomposites for Corrosion Protection and Bioactivity. Baghdad Science Journal. 2023.
17. Zheng J, Liu L, Ji G, Yang Q, Zheng L, Zhang J. Hydrogenated Anatase $TiO_2$ as Lithium-Ion Battery Anode: Size–Reactivity Correlation. ACS Applied Materials and Interfaces. 2016;8(31):20074-20081.
18. Aisyah N, Rifai H, Maisonneuve CBDL, Oalmann J, Forni F, Eisele S, et al. Scanning electron microscope (SEM) imaging and analysis of magnetic minerals of lake Diatas peatland section DD REP B 693. Journal of Physics: Conference Series. 2020;1481(1):012025.
19. Hosseini MG, Bagheri R, Najjar R. Electropolymerization of polypyrrole and polypyrrole-ZnO nanocomposites on mild steel and its corrosion protection performance. J Appl Polym Sci. 2011;121(6):3159-3166.
20. García-Galvan FR, Fajardo S, Barranco V, Feliu S. Experimental Apparent Stern–Geary Coefficients for AZ31B Mg Alloy in Physiological Body Fluids for Accurate Corrosion Rate Determination. Metals. 2021;11(3):391.
21. Mohammed RA, Saleh KA. Electropolymerization of [N-(1, 3-thiazo-2-yl)] maleamic acid and their Nanocomposite with Graphene Oxide as Protective Coating against Corrosion and Antibacterial Action. Iraqi Journal of Science. 2022:4163-4174.
22. Karimi A, Danaee I, Eskandari H, RashvanAvei M. Electrochemical investigations on the inhibition behavior and adsorption isotherm of synthesized di-(Resacetophenone)-1,2-cyclohexandiimine Schiff base on the corrosion of steel in 1 M HCl. Protection of Metals and Physical Chemistry of Surfaces. 2015;51(5):899-907.
23. Mohammed Ali Al-Sammarraie A, Hasan Raheema M. Electrodeposited Reduced Graphene Oxide Films on Stainless Steel, Copper, and Aluminum for Corrosion Protection Enhancement. International Journal of Corrosion. 2017;2017:1-8.
24. Solomon MM, Umoren SA, Udosoro II, Udoh AP. Inhibitive and adsorption behaviour of carboxymethyl cellulose on mild steel corrosion in sulphuric acid solution. Corros Sci. 2010;52(4):1317-1325.
25. Bentiss F, Bouanis M, Mernari B, Traisnel M, Vezin H, Lagrenée M. Understanding the adsorption of 4 H -1,2,4-triazole derivatives on mild steel surface in molar hydrochloric acid. Appl Surf Sci. 2007;253(7):3696-3704.
26. Al-Mashhadani HA, Saleh KA. Electro-polymerization of poly eugenol on ti and ti alloy dental implant treatment by micro arc oxidation using as anti-corrosion and anti-microbial. Research Journal of Pharmacy and Technology. 2020;13(10):4687.